

# Dual-specificity phosphatase 5 controls the localized inhibition, propagation, and transforming potential of ERK signaling

Kidger, Andrew M.; Rushworth, Linda K.; Stellzig, Julia; Davidson, Jane; Bryant, Christopher J.; Bayley, Cassidy; Caddye, Edward; Rogers, Tim; Keyse, Stephen M.; Caunt, Christopher J.

*Published in:*
Proceedings of the National Academy of Sciences of the United States of America

*DOI:*
10.1073/pnas.1614684114

*Publication date:*
2017

*Document Version*
Peer reviewed version

# DUSP5 controls the localized inhibition, propagation and transforming potential of ERK signaling

**Andrew Kidger[a,1], Linda Rushworth[a,1], Julia Stellzig[a], Jane Davidson[a], Christopher Bryant[b], Cassidy Ann Bayley[b], Edward Caddye[b], Tim Rogers[c], Stephen Keyse[a,2] and Christopher James Caunt[b,2]**

[a]Stress Response Laboratory, Division of Cancer Research, Jacqui Wood Cancer Centre, Ninewells Hospital & Medical School, University of Dundee, Dundee DD1 9SY, United Kingdom. [b]Department of Biology and Biochemistry, University of Bath, Claverton Down, Bath BA2 7AY, United Kingdom, [c]Department of Mathematics, University of Bath, Claverton Down, Bath BA2 7AY, United Kingdom [1]These authors contributed equally to this work. [2]Corresponding authors: c.caunt@bath.ac.uk and s.m.keyse@dundee.ac.uk

Submitted to Proceedings of the National Academy of Sciences of the United States of America

**Deregulated ERK signaling drives cancer growth. Normally, ERK activity is self-limiting by the rapid inactivation of upstream kinases and delayed induction of dual-specificity MAP kinase phosphatases (MKPs/DUSPs). However, interactions between these feedback mechanisms are unclear. Here we show that while the MKP, DUSP5, both inactivates and anchors ERK in the nucleus, it paradoxically increases and prolongs cytoplasmic ERK activity. The latter effect is caused, at least in part, by the relief of ERK-mediated RAF inhibition. The importance of this spatiotemporal interaction between these distinct feedback mechanisms is illustrated by the fact that expression of oncogenic BRAF$^{V600E}$, a feedback-insensitive mutant RAF kinase, reprograms DUSP5 into a cell-wide ERK inhibitor that facilitates cell proliferation and transformation. In contrast, DUSP5 deletion causes BRAF$^{V600E}$-induced ERK hyperactivation and cellular senescence. Thus, feedback interactions within the ERK pathway can regulate cell proliferation and transformation, and suggest oncogene-specific roles for DUSP5 in controlling ERK signaling and cell fate.**

ERK | MAPK | MKP | DUSP | Signaling

## Introduction

Activation of the prototypic MAPK (mitogen-activated protein kinase), ERK (extracellular signal-regulated kinase), regulates a range of cell fate decisions including differentiation, proliferation and death (1, 2). Most stimuli engage ERK signaling by activating RAS GTPases, which promote the dimerization and activation of RAF kinases. RAF then phosphorylates and activates MEK (MAPK/ERK kinase), which in turn phosphorylates both threonine and tyrosine residues within a signature T-E-Y motif to activate ERK (2, 3). Under physiological conditions, ERK activity is self-limiting by the rapid phosphorylation and inhibition of upstream components, such as RAF kinases (4–6), RAS exchange factors (7) and receptor tyrosine kinases (RTKs) (8, 9), but also by delayed induction of dual-specificity MAP kinase phosphatases (MKPs/DUSPs), which dephosphorylate and inactivate ERK (10, 11). Whether these temporally distinct negative feedback loops have cooperative or distinct roles in regulating ERK signaling is currently unclear.

Oncogenic mutations in RAS (RAS$^{mut}$) or a V600E substitution in BRAF frequently drive tumor progression through constitutive downstream MEK-ERK activation (12). ERK-inhibitory proteins, such as the MKP/DUSPs, are therefore often assumed to be tumor suppressors, but both decreased and increased MKP/DUSP expression is linked to tumor progression in different contexts (13). These observations may, at least in part, be explained by evidence showing that high intensity ERK activation in some cell and tumor types engages tumor suppressive mechanisms, such as senescence (14–18). In such circumstances, the attenuation of ERK signaling by MKP/DUSPs may actually promote tumor progression (16, 17).

DUSP5, a nuclear-localized member of the MKP/DUSP family, is induced in response to ERK activation (19, 20) and specifically dephosphorylates and anchors ERK in the nucleus (21). We recently established that *Dusp5* knockout (KO) mice are sensitized to HRAS$^{Q61L}$-driven DMBA/TPA (7,12-Dimethylbenz[a]anthracene/12-*O*-tetra-decanoylphorbol-13-acetate)-initiated skin carcinogenesis, due to increased nuclear ERK activity and ERK-dependent SerpinB2 expression (22). Furthermore, the downregulation of DUSP5 in gastric and prostate cancers is also associated with a poor prognosis (23, 24), suggesting that DUSP5 can function as a tumor suppressor. In contrast, DUSP5 expression is commonly retained or even enhanced in BRAF$^{V600E}$-driven colorectal, melanoma and thyroid cancer cell lines and tumors (25–27). This suggests that DUSP5 may either promote or limit the oncogenic potential of ERK signaling, depending on cellular context.

Here, we report that in addition to its role in the nuclear inactivation of ERK, DUSP5 increases RAF, MEK and ERK activity in the cytoplasm. This latter effect is caused by the relief of upstream kinase inhibition, and depends on both the turnover rate of DUSP5 and its ability to sequester inactive ERK in the nucleus. Expression of the BRAF$^{V600E}$ oncoprotein, which is insensitive to feedback inhibition, alters the function of DUSP5 to become a cell-wide inhibitor of ERK, which in turn enables cells to avoid ERK hyperactivation and senescence. These data may explain why DUSP5 may be associated with tumor suppression or promotion in different tumor types.

### Significance

**The RAF-ERK kinase pathway drives cell proliferation and cancer growth. ERK kinase activity is terminated by dual-specificity MAPK phosphatases (MKP/DUSPs), which are often assumed to be tumor suppressors. We demonstrate that the MKP, DUSP5, terminates nuclear ERK signaling, but surprisingly promotes ERK activation in the cytoplasm by relieving feedback inhibition of upstream kinases. Cancer-causing RAF kinase mutations, which occur in ~8% of tumors and are refractory to feedback inhibition, reprogram DUSP5 to become a cell-wide attenuator of ERK signaling that prevents cellular senescence and promotes oncogenic transformation. Our results establish that interactions between feedback loops in the ERK cascade control localized signal-promotion or suppression, which in turn govern cell proliferation and transformation.**

**Reserved for Publication Footnotes**

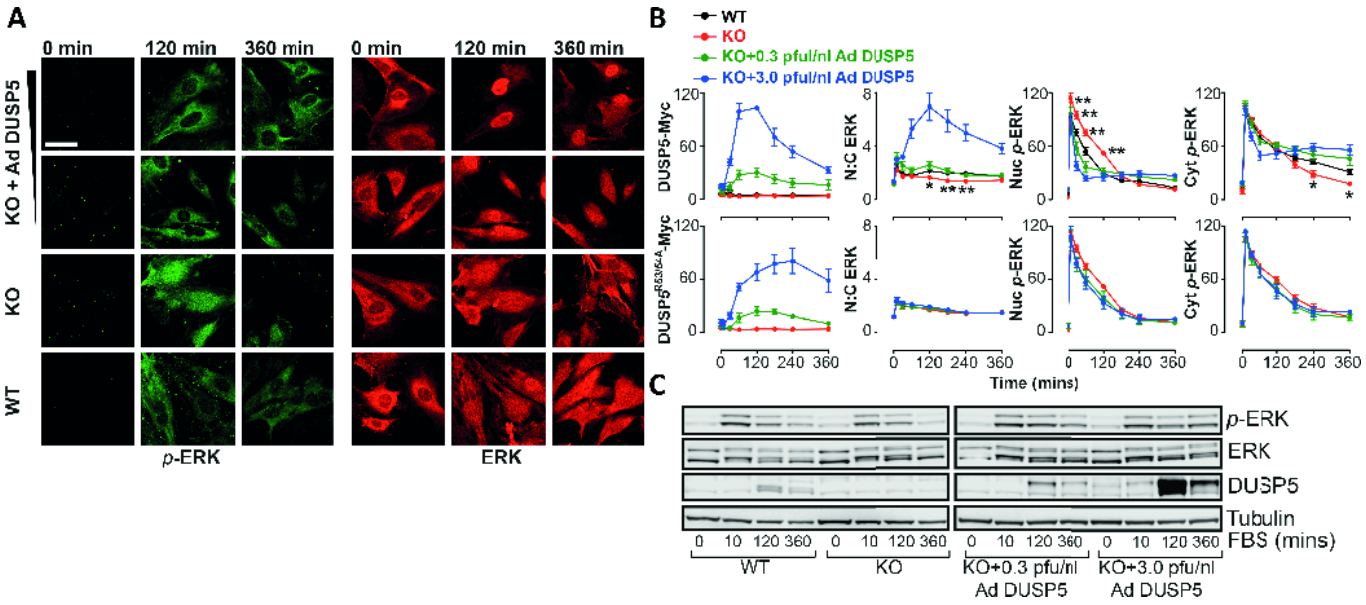




**Fig. 1.** DUSP5 propagates cytoplasmic ERK signaling. Serum-starved primary MEFs from wild-type (WT) or DUSP5 knockout (KO) mice were infected with either 0.3-3.0 pfu/nl Ad ERK-responsive *EGR1* promoter-driven DUSP5-Myc (DUSP5) or a KIM mutant of DUSP5-Myc (DUSP5$^{R53/54A}$) and stimulated with 20% FBS for times indicated. (*A*) Representative confocal images of *p*-ERK and ERK are shown. Scale bar = 60 μm. (*B*) High content microscopy was used to quantify >$10^4$ cells per condition, per experiment for levels of Myc tag, nuclear (Nuc) or cytoplasmic (Cyt) *p*-ERK intensity, or nuclear:cytoplasmic ratio (N:C) of total ERK fluorescence. Data are normalized mean AFU values ±SEM, n = 4-8, *p<0.05, **p<0.01 comparing WT vs KO using 2-way repeated measures ANOVA and Bonferroni post-test. *Note*: KO data are identical in upper and lower plots. (*C*) Western blots of whole cell lysates are shown for total and TEY activation loop phosphorylated (*p*-) ERK, β-tubulin and DUSP5. A representative blot is shown from n=3 similar experiments; blot quantification is shown in Fig. S1C.

## Results

**DUSP5 controls both nuclear and cytoplasmic ERK activity.** We have previously demonstrated that DUSP5 causes both nuclear accumulation and dephosphorylation of ERK in mouse embryonic fibroblasts (MEFs) when stimulated with the phorbol ester, TPA (22). These localized effects were revealed using confocal and high content microscopy (HCM) (22). We therefore used similar methodology to compare the effects of DUSP5 on ERK responses to serum and growth factors.

Fetal bovine serum (FBS) stimulation of serum-starved primary wild-type (WT) MEFs rapidly elicited high levels of dually (pT-E-pY) phosphorylated ERK (*p*-ERK) in the nucleus and cytoplasm (from 5-60 min), followed by nuclear dephosphorylation of ERK and a prolonged phase (120-360 min) of lower-intensity cytoplasmic *p*-ERK signaling (~30-50% of peak values) (Fig. 1A, 1B, S1A and S1B). This is consistent with studies in several cell types showing that prolonged growth factor or serum stimulus typically causes transient nuclear but sustained cytoplasmic ERK activation (28, 29). Maximal increases in ERK nuclear accumulation (reflected by the nuclear:cytoplasmic, N:C, ratio of total ERK) occurred concurrently with the onset of nuclear ERK dephosphorylation, (Fig. 1A, 1B and S1B) and DUSP5 expression (Fig. 1C), suggesting that DUSP5 may be responsible for the nuclear accumulation and dephosphorylation of ERK (21, 22). In agreement with this hypothesis, *Dusp5* deletion both reduced the N:C ERK ratio and elevated nuclear *p*-ERK levels (Fig. 1A, 1B and S1A). Surprisingly, *Dusp5* deletion also reduced the amplitude of the prolonged (240-360 min) serum-induced cytoplasmic *p*-ERK response, suggesting that in addition to its nuclear inactivation of ERK, DUSP5 may also promote cytoplasmic ERK activation (Fig. 1A and 1B).

Previous reports show that constitutive overexpression of DUSP5 causes the constitutive nuclear accumulation and dephosphorylation of ERK (21). We therefore hypothesized that the propagation of cytoplasmic *p*-ERK levels (Fig. 1A and B) may arise because DUSP5 is induced in response to ERK activity (19, 20). To test this, we rescued DUSP5 expression in *Dusp5* KO MEFs using adenovirus (Ad) vectors containing an ERK-responsive 1.2 kb *EGR1* immediate early gene promoter to drive DUSP5-Myc expression (22). Low titer (0.3 pfu/nl) Ad DUSP5-Myc restored transient DUSP5 expression (Fig. 1C), as well as corresponding changes ERK N:C ratio, ERK nuclear dephosphorylation and the cytoplasmic rebound in *p*-ERK (Fig. 1A, 1B, and S1). The addition of higher titer Ad DUSP5-Myc (up to 3 pfu/nl) caused supraphysiological DUSP5 expression (Fig. 1C) and exaggerated all endpoints of ERK regulation, including the propagation of cytoplasmic ERK activity (Fig. 1A, 1B, and S1B). These effects of *Dusp5* KO and rescue on cytoplasmic *p*-ERK were also reflected in Western blots of whole cell lysates, most likely because the cytoplasm occupies a much greater volume of MEFs than the nucleus (compare Fig. 1B, 1C and S1C). Negative control experiments using Ad to express an R53/54A kinase interaction motif (KIM) mutant of DUSP5-Myc that is unable to bind to ERK and driven by the same *EGR1* promoter (21, 22), failed to influence ERK responses at any titer, indicating the necessity of DUSP5 association with ERK (Fig. 1B and S1B). Plotting of single cell data revealed that increased cytoplasmic *p*-ERK levels after 240 min FBS stimulus correlated with increases in both DUSP5-Myc (but not DUSP5$^{R53/54A}$-Myc) expression levels and ERK N:C ratio, indicating that these effects are cell-autonomous (Fig. S2).

Our previous studies, using TPA stimulation of MEFs without serum starvation, showed that endogenous levels of DUSP5 suppressed nuclear ERK activity, but did not alter cytoplasmic *p*-ERK responses (22). We repeated these experiments, but included Ad DUSP5-Myc or Ad DUSP5$^{R53/54A}$-Myc to rescue expression from sub- to supraphysiological levels in *Dusp5* KO MEFs. DUSP5-Myc, but not DUSP5$^{R53/54A}$-Myc, caused dose-dependent nuclear dephosphorylation and anchoring of ERK in response to TPA, but cytoplasmic *p*-ERK responses were only increased at supraphysiological levels of DUSP5 (Fig. S3A). DUSP5-Myc over-expression also increased cytoplasmic *p*-ERK responses to nerve growth factor (NGF) stimulation in rat PC12 cells (Fig. S3B). These data collectively indicate a novel function

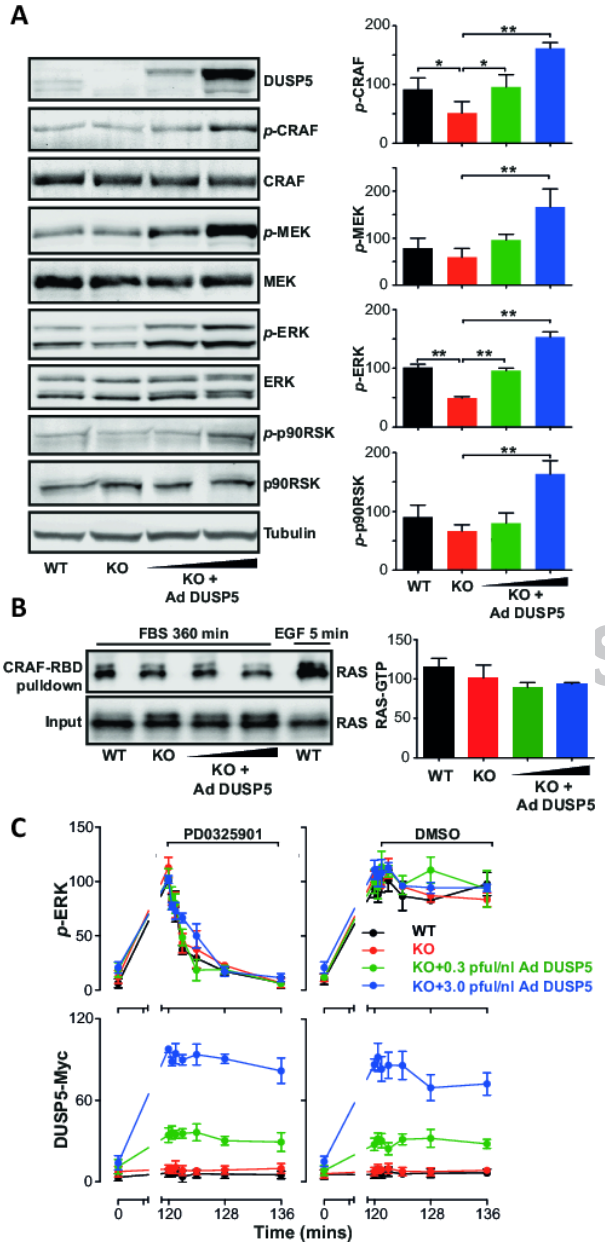


**Fig. 2.** DUSP5 propagates ERK signaling by increasing RAF and MEK activity.Wild-type (WT) and *Dusp5* knockout (KO) primary MEFs were infected with 0.3-3.0 pfu/nl Ad *EGR1* promoter-driven DUSP5-Myc (Ad DUSP5) as indicated. (*A*) MEFs were stimulated for 360 min with 20% FBS. Western blots of whole cell lysates were probed for phospho (*p*-) sites on ERK (TEY activation loop), MEK (Ser217/221), CRAF (Ser338) and p90RSK (Thr 359/Ser363) as well as total kinase levels and β-tubulin. Normalized blot quantification is shown ±SEM, n = 4. *p<0.05, **p<0.01 comparing KO vs all columns using 1-way ANOVA and Dunnett's post-test. (*B*) MEFs were stimulated either with 20% FBS for 360 min or 50 ng/ml EGF for 5 min prior to lysis and pull down of GTP-RAS using the RAS-binding domain (RBD) of CRAF. Input levels of total RAS in whole cell lysates and levels of GTP-RAS in the pull down were measured by Western blotting. Normalized mean blot quantification of GTP-RAS is shown ±SEM, n = 3. (*C*) MEFs were stimulated with 20% FBS for 120 min prior to addition of either DMSO vehicle or 5 μM PD0325901 MEK inhibitor for times indicated. Levels of Myc-tag and whole-cell levels of *p*-ERKwere measured using high content microscopy. Data shown are normalized population AFU values, n=3, ±SEM.

of DUSP5 - the maintenance or propagation of cytoplasmic *p*-ERK signaling - that is cell autonomous, dose-dependent and reliant upon association with ERK via the KIM domain.

**DUSP5 propagates ERK signaling by increasing RAF and MEK activation.** To determine how DUSP5 may cause increased ERK signaling, we examined the effects of *Dusp5* deletion and rescue on the core ERK pathway components; CRAF, MEK and ERK, as well as the ERK substrate, p90 ribosomal S6 kinase (p90RSK), after 360 min FBS stimulus. Whilst only *p*-ERK levels showed a very obvious and substantial reduction in levels following *Dusp5* deletion, *p*-CRAF levels were also significantly reduced, and Ad DUSP5-Myc rescue caused clear and dose-dependent increases in the levels of all four phospho kinases measured (Fig. 2A). It is likely that the more readily detectable differences in *p*-ERK levels reflects the greater relative abundance of ERK compared to the other kinases and because of signal amplification through the RAF-MEK-ERK cascade (30). Comparisons of MEK and ERK responses to FBS in fractionated lysates showed that DUSP5 significantly increased cytoplasmic *p*-MEK levels without influencing its localization or expression, while *p*-ERK responses echoed those observed in our microscopy assays (compare Fig. S4 and Fig. 1B). Strikingly, DUSP5 did not influence FBS-induced RAS activation, even when expressed at supraphysiological levels (Fig 2B). In contrast, elevated RAS-GTP was readily detected in positive control samples stimulated with epidermal growth factor (EGF) for 5 min (Fig. 2B). Whilst it is possible that there could be highly localized or subtle changes in RAS activation that we cannot measure in whole cell lysates, the data suggest that DUSP5 causes major effects on ERK phosphorylation by promoting pathway activity *downstream* of RAS.

To investigate the possibility that DUSP5 could also promote ERK activity by attenuating other ERK phosphatases, we compared the rate of ERK dephosphorylation after 120 min FBS stimulus and addition of a specific MEK inhibitor (MEKi), PD0325901, under conditions of *Dusp5* deletion and rescue. A complete loss of *p*-ERK was observed within 8 min following MEKi addition, irrespective of DUSP5 expression level (Fig. 2C). We were also unable to detect differences in *p*-ERK half-life under these conditions, which is likely due to the very high constitutive rates of ERK dephosphorylation observed even in the absence of DUSP5 expression. These results exclude the possibility that DUSP5 could promote *p*-ERK signaling over several hours by attenuating the activity of other ERK phosphatases, and indicate that continuous MEK activity is required for the propagation of ERK signaling by DUSP5. These data are also supported by our previous studies showing that *Dusp5* KO does not change either serum or TPA-induced expression of other ERK-regulatory MKP/DUSPs in MEFs (DUSP4, 6, 7 and 9) (22).

Knock-down of DUSP5 in some cancer cell lines has been reported to influence AKT phosphorylation (31), suggesting DUSP5 may influence additional RAS-effector pathways. We therefore compared FBS-induced activation of the ERK and PI3K-AKT pathways by measuring *p*-AKT and *p*-ERK levels in *Dusp5* KO and rescue experiments. Whilst *p*-ERK levels were again increased by DUSP5-Myc expression, *p*-AKT levels were unchanged in the same cells, indicating that in MEFs, the effects of DUSP5 are unlikely to be mediated by changes in the activity of this alternative RAS effector pathway (Fig. S3C). These results are also consistent with our previous studies showing that *Dusp5* deletion does not influence JNK or p38 MAPK responses to FBS or TPA stimuli (22). Thus, DUSP5 is most likely able to increase the cytoplasmic activity of RAF, MEK and ERK without invoking pathway cross-talk.

**DUSP5 nuclear localization controls cytoplasmic ERK phosphorylation.** Our experiments revealing that DUSP5 can prolong ERK signaling raise the question of whether other MKP/DUSPs might also exhibit this behavior. DUSP6 (also known as MKP-3/Pyst1) is analogous to DUSP5 in its ERK-dependent promoter regulation (32), ERK substrate specificity (33), sequestration of ERK (34) and rate of turnover (20, 35), but is localized in the

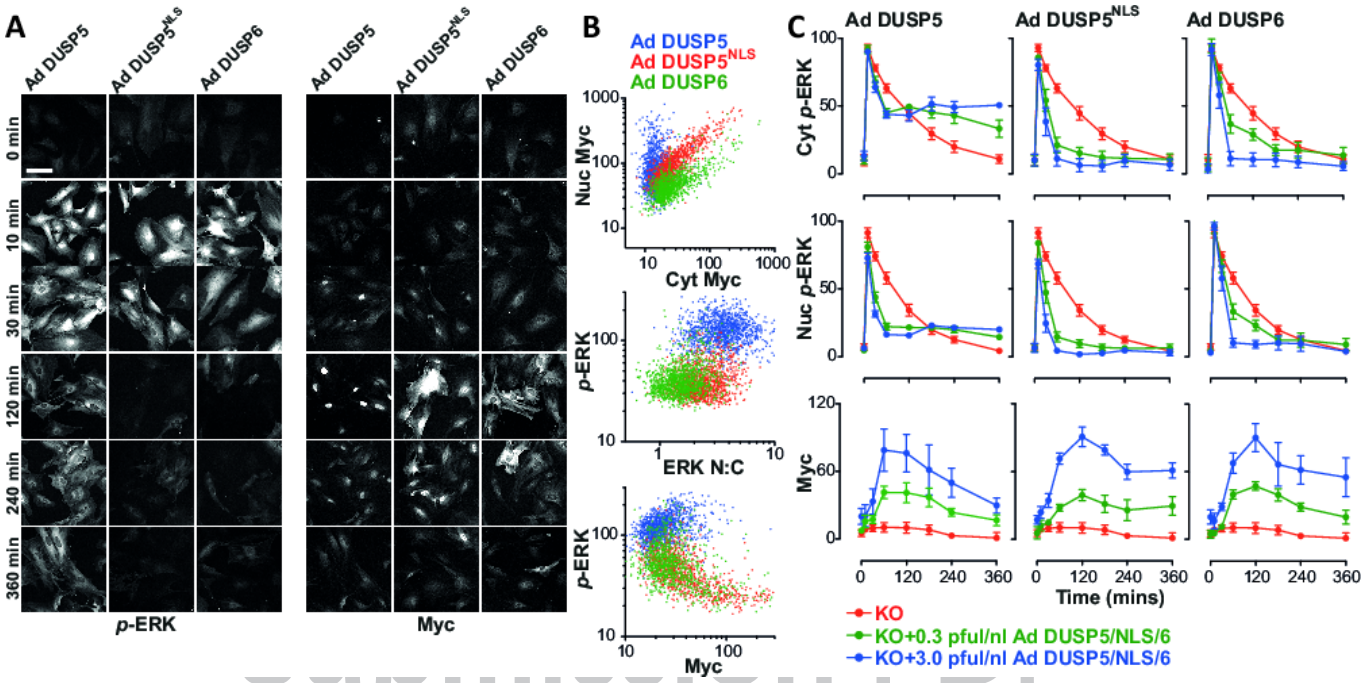


**Fig. 3.** The DUSP5 nuclear localization signal is required for propagation of cytoplasmic *p*-ERK. Primary *Dusp5* knockout (KO) MEFs were infected with 0.3-3 pfu/nl Ad *EGR1* promoter-driven DUSP5-Myc (Ad DUSP5), a nuclear localization sequence mutant of DUSP5-Myc or DUSP6-Myc (Ad DUSP5$^{NLS}$ and Ad DUSP6, respectively), and stimulated with 20% FBS. (*A*) Representative high content microscopy images show cells infected with 3 pfu/nl Ad DUSP-Myc prior to stimulation and staining for both TEY phosphorylated (*p*-) ERK and Myc-tag. <1% imaged area per condition per experiment is shown. Scale bar = 100 μm. (*B*) Scatterplots show single cell comparisons of nuclear versus cytoplasmic levels of Myc tag (top), whole-cell Myc-tag versus whole-cell *p*-ERK levels (middle) or ERK nuclear:cytoplasmic (N:C) ratio versus whole-cell *p*-ERK levels, from a single representative experiment of n = 4 comparing cells infected with 3 pfu/nl Ad DUSP and stimulated for 180 min with FBS. All non-ratio values are shown in raw AFU per cell. (*C*) Plots show average nuclear (Nuc) *p*-ERK, cytoplasmic (Cyt) *p*-ERK and whole cell Myc levels in cells stimulated with FBS. Data shown are mean, normalized AFU levels ±SEM, n = 4. *Note*: KO data are identical in each row and are shown in each plot to clarify the effects of Ad DUSP-Myc expression in the *Dusp5*-deleted cells.

cytoplasm due to an N-terminal nuclear export sequence (33, 34), while a nuclear localization sequence (NLS) close to the KIM causes DUSP5 to accumulate in the nucleus (21).

To test whether DUSP5 effects on cytoplasmic *p*-ERK were dependent on its nuclear localization, we used the *EGR1* promoter in identical Ad backbone vectors to enable a direct comparison of DUSP5-Myc with DUSP6-Myc or an NLS mutant of DUSP5-Myc (DUSP5$^{NLS}$), which impedes nuclear import but maintains catalytic and anchoring functions (21). FBS stimulation of *Dusp5* KO cells infected with Ad DUSP5-Myc, DUSP5$^{NLS}$-Myc or DUSP6-Myc induced comparable levels of expression but with different localization; DUSP5-Myc was almost exclusively nuclear, DUSP6-Myc was chiefly cytoplasmic, while DUSP5$^{NLS}$-Myc was evenly distributed (Fig. 3A and 3B), which is consistent with previous reports using these ORFs driven by constitutive promoters (21, 34). As expected, DUSP5-Myc expression led to elevated ERK N:C ratio, but maintained high levels of *p*-ERK per cell (Fig. 3B). Consistent with their ability to inactivate and sequester ERK in their respective cellular locations, DUSP5$^{NLS}$-Myc and DUSP6-Myc reduced *p*-ERK and also the ERK N:C ratio (Fig. 3B). To determine if the differential effects of these DUSP-Myc transgenes could be due to altered expression kinetics, we compared time courses of *p*-ERK responses to FBS at varied Ad titers. Each of the DUSP-Myc proteins showed comparable magnitude and kinetics of induction, but only DUSP5-Myc was able to propagate cytoplasmic ERK activity. In contrast, both DUSP5$^{NLS}$-Myc and DUSP6-Myc potently and dose-dependently decreased *p*-ERK throughout the cell (Fig. 3A and 3C). These data suggest that DUSP5-mediated increases in cytoplasmic *p*-ERK are dependent upon its nuclear localization.

**DUSP5 propagates ERK signaling by relieving upstream kinase inhibition.** A major mechanism by which ERK self-limits its activity is through direct phosphorylation and inhibition of upstream components, such as RAS exchange factors (7), RTKs (8, 9) and RAF kinases, which prevent RAS-mediated RAF dimerization and activation (4–6). This rapid negative feedback confers homeostatic control, such that pharmacological inhibition or a reduction in total ERK concentration cause strong compensatory increases in upstream kinase activity, which acts to maintain near constant *p*-ERK output levels (30, 36, 37). We therefore hypothesized that the nuclear sequestration and inactivation of ERK by DUSP5 may cause similar compensatory increases in upstream kinase activity, and that this may explain why cytoplasmic *p*-ERK levels are maintained or even prolonged in the presence of DUSP5.

To assess whether our hypothesis was tenable, we devised a simplified mathematical model to explore the nature of interactivity between DUSP5, ERK and upstream kinases that could cause DUSP5 to increase ERK signaling (Fig. 4A). In this network, K (representing all kinases upstream of ERK), is converted upon stimulus to an activated form, K*, which catalyzes the conversion of ERK to an active form, ERK*. To replicate typical receptor signaling, we modeled the conversion of K to K* as being rapid, followed by slower exponential conversion back to K. To represent rapid feedback inhibition of upstream kinases, ERK* was able to accelerate the deactivation of K* in our model (Fig. 4A, S5A and SI Materials and Methods). Previous studies indicate that ERK-mediated inhibition of RAF is chiefly responsible for homeostatic control of the ERK cascade, and is highly non-linear in nature (30, 36, 37). We therefore modeled the relationship between ERK* and K* as highly cooperative by using a Hill function with a Hill coefficient of 4 (SI Materials

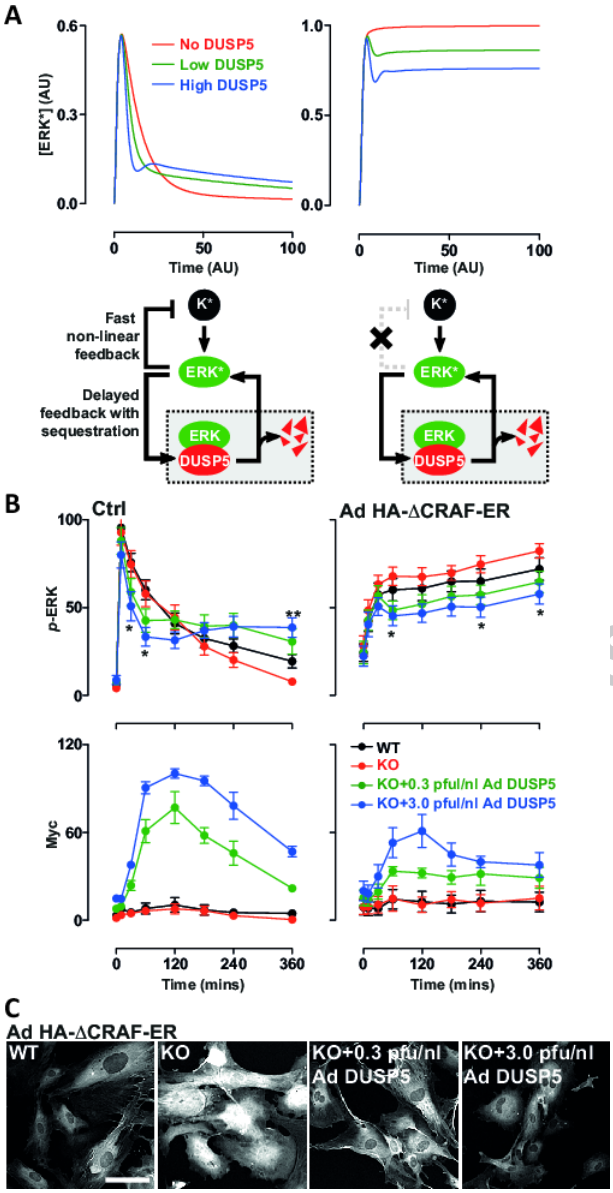


**Fig. 4.** DUSP5 propagates ERK signaling by relieving upstream kinase inhibition. (*A*) The cartoons show conceptual model network structures comprising ERK activation by an upstream kinase (K), feedback inhibition and sequestration of ERK by DUSP5, and non-linear feedback inhibition of K by ERK. K* and ERK* denote activated forms of K and ERK, respectively. The plots show model predictions of ERK* concentration versus time in arbitrary units (AU) under conditions where there is 'No', 'Low' or 'High' levels of DUSP5 and in which negative feedback between ERK and K is intact (left) or completely disabled (right). (*B*) Wild-type (WT) and *Dusp5* knockout (KO) MEFs were infected with either empty Ad, or Ad expressing HA-ΔCRAF-ER, alongside either 0.3 or 3 pfu/nl of Ad *EGR1* promoter-driven DUSP5-Myc. Cells were stimulated with either 20% FBS (left) or 0.1 μM 4HT (right) prior to immunostaining for TEY phosphorylated (*p*-) ERK and Myc-tag followed by high content microscopy analysis. Normalized population mean AFU values for whole-cell *p*-ERK and Myc intensity are shown ±SEM, n=6, *p<0.05, **p<0.01 comparing KO vs KO+3.0 pfu/nl Ad DUSP5-Myc using 2-way repeated measures ANOVA and Bonferroni post-test. (*C*) Representative high content microscopy images are shown from experiments described in (*B*), comparing Ad HA-ΔCRAF-ER-infected MEFs after 360 min stimulus with 0.1 μM 4HT. Scale bar = 100 μm

and Methods). As ERK induces DUSP5 expression (19, 20), we modeled DUSP5 synthesis as dependent upon ERK*, but with a delay to replicate the time lag incurred by transcription and translation. Because DUSP5 differentially controls nuclear and cytoplasmic ERK activity (Fig. 1), we initially included compartmentalization and ERK traffic in our model (SI Materials and Methods). However, biological rates of ERK nuclear shuttling are fast enough relative to the time scale of *p*-ERK propagation, that their inclusion in the model did not influence *in silico* predictions (Fig. S5B). Therefore, in our model we assumed for simplicity that all ERK associated with DUSP5 is inactive and that the release of inactive ERK occurs through DUSP5 degradation (Fig. 4A and SI Materials and Methods).

When K, ERK and DUSP5 enzymes were linked this way *in silico*, increasing DUSP5 levels proportionally increased the ERK* response (Fig. 4A), which qualitatively replicated the kinetics of FBS-induced *p*-ERK responses observed in cells, using *Dusp5* KO and rescue experiments in MEFs (Fig. 4B). Reducing the cooperativity of feedback between ERK* and K* in our mathematical model caused reduced the ability of DUSP5 to propagate ERK* (Fig. S5A), while complete disruption of feedback between ERK* and K* completely reversed DUSP5 function, such that increasing DUSP5 levels proportionally reduced ERK* (Fig. 4A, compare left and right plots). These mathematical simulations suggest that the effects of DUSP5 are reliant upon the relief of upstream feedback mechanisms. To test this prediction, we generated Ad expressing an HA-tagged fusion protein of the conserved region 3 (CR3) kinase domain of CRAF (residues 305-648), and the estrogen receptor ligand-binding domain (HA-ΔCRAF-ER). The CR3 region of CRAF lacks five (of six) inhibitory ERK phosphorylation sites (4), and is therefore insensitive to feedback inhibition (30). HA-ΔCRAF-ER also lacks an N-terminal auto-inhibitory domain, while the fusion to ER renders it conditionally activatable by the addition of 4-hydroxytamoxifen (4HT) (38). Accordingly, stimulation of MEFs expressing HA-ΔCRAF-ER with 4HT caused rapid, sustained increases in *p*-ERK (Fig. 4B and C). Under these conditions, DUSP5 dose-dependently reduced *p*-ERK levels in both the nucleus and cytoplasm, mimicking the predictions generated in our mathematical model (compare Fig. 4A, B and C). These data indicate that key aspects of DUSP5 function, and specifically its ability to promote ERK activity, are dependent upon the relief of upstream negative feedback within the ERK cascade.

**DUSP5 degradation controls the amplitude and duration of ERK activity**. Published estimates of DUSP5 half-life are in the order of ~45 min (20), but how this rapid turnover influences ERK regulation is unclear. We employed our mathematical model to predict the effects of altering DUSP5 half-life, and found that abrogating DUSP5 degradation reduced the amplitude of sustained ERK* signaling *in silico* (Fig. 5A). To test this prediction, we reconstituted *Dusp5* KO MEFs with supraphysiological levels of either DUSP5-Myc or DUSP5$^{R53/54A}$-Myc, and used a proteasome inhibitor (MG132) to block DUSP5 degradation 120 min after FBS stimulation. MG132 blocked the degradation of DUSP5-Myc and caused a corresponding increase in ERK nuclear accumulation (ERK N:C ratio; Fig. 5B), but reduced *p*-ERK signal propagation by up to 50% (Fig. 5B and 5C). In contrast, DUSP5$^{R53/54A}$-Myc did not influence *p*-ERK responses or ERK N:C ratio, replicating the 'No DUSP5' conditions in our mathematical model (Fig. 5B). Importantly, MG132 addition to cells expressing DUSP5$^{R53/54A}$-Myc did not influence *p*-ERK signaling, indicating that its effects in cells expressing DUSP5-Myc arise specifically because the interaction between ERK and DUSP5 is prolonged (Fig. 5B). Controls using MEKi addition after 120 min reduced *p*-ERK and ERK N:C to basal levels within minutes, indicating that continuous MEK activity is required for DUSP5 to propagate ERK signaling and cause continuous ERK nuclear accumulation (Fig. 5B). Taken together, these data support a model where DUSP5 firstly sequesters dephosphorylated ERK in the nucleus, causing a relief of upstream

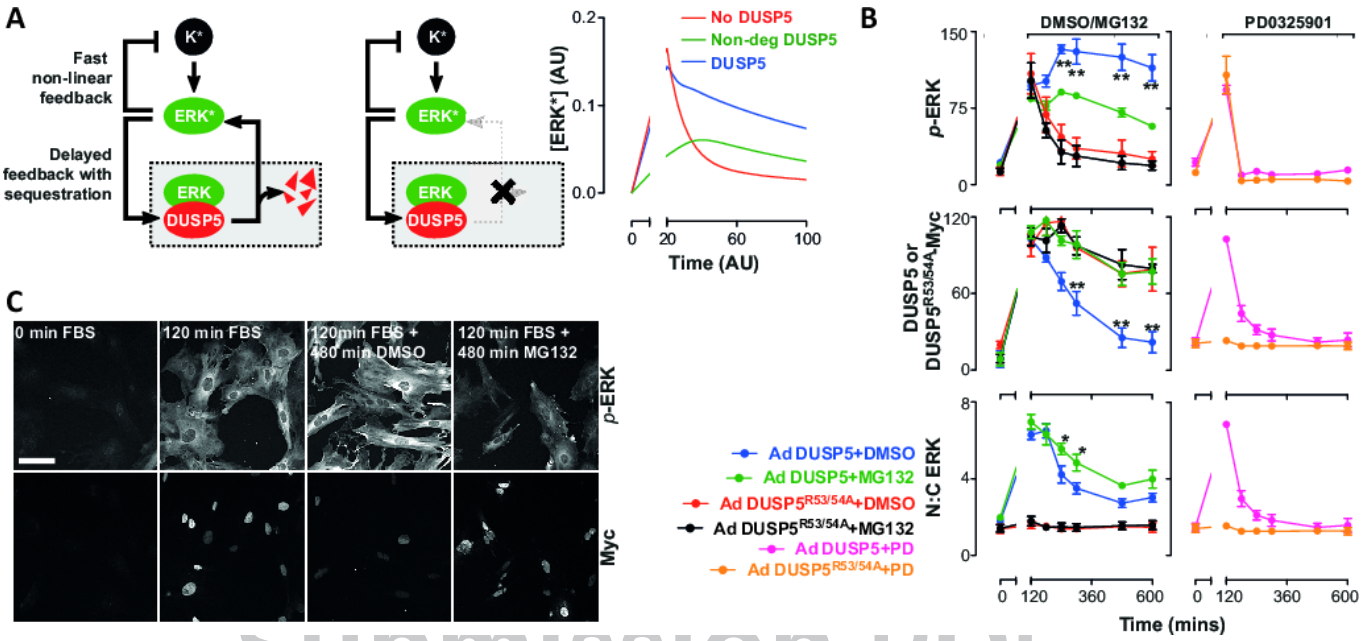




**Fig. 5.** DUSP5 degradation controls the amplitude and duration of ERK signaling.(*A*) The cartoons depict a 'normal' network structure (left) and one in which DUSP5 degradation is abrogated (right). The plot compares model simulations for conditions where DUSP5 is synthesized and degraded (DUSP5), where DUSP5 is absent (No DUSP5) or synthesized but not degraded (Non-deg DUSP5). Comparisons of activated ERK (ERK*) concentrations versus time are shown in arbitrary units (AU). *Note*: the break in the x-axis is to enable direct comparison with the wet-lab data shown in (*B*), in which only prolonged phases (>120 min) of FBS stimulus were measured. (*B*) *Dusp5* knockout (KO) MEFs were infected with 3 pfu/nl of adenovirus (Ad) expressing *EGR1*-promoter driven DUSP5-Myc or DUSP5$^{R53/54A}$-Myc prior to 20% FBS stimulus for 120 min and treatment with either DMSO vehicle, 10 μM MG132 proteasome inhibitor, or 5 μM PD0325901 MEK inhibitor (PD). Plots show high content microscopy readouts for whole-cell *p*-ERK, ERK nuclear:cytoplasmic ratio (N:C) and whole-cell Myc intensity and are shown as normalized population mean AFU ±SEM, n=3. *p<0.05, **p<0.01 using 2-way ANOVA and Bonferroni post-test comparing DMSO and MG132-treated cells.(*C*) Representative images are shown from high content microscopy experiments described in (*B*). Scale bar = 100 μm.

kinase inhibition, and that the subsequent degradation of DUSP5 releases ERK from the nucleus, causing a rebound in *p*-ERK levels.

**DUSP5 facilitates BRAF$^{V600E}$-driven cell proliferation and transformation.** The oncogenic V600E substitution in BRAF causes constitutive kinase activation, irrespective of RAS activation or dimerization status (5). As such, BRAF$^{V600E}$ is refractory to feedback inhibition by ERK (26, 30, 36, 37). In contrast, RAS$^{mut}$ oncoproteins constitutively activate the ERK pathway, but leave ERK-RAF negative feedback intact. We therefore hypothesized that DUSP5 would cause more profound effects on *p*-ERK signaling in the presence of BRAF$^{V600E}$ than RAS$^{mut}$. To test this, we expressed comparable levels of HA-BRAF$^{V600E}$ or HA-HRAS$^{Q61L}$ in WT and *Dusp5* KO MEFs (Fig. S6) prior to FBS stimulation, and rescued DUSP5-Myc expression to normal or supraphysiological levels. In control cells lacking oncogene expression, DUSP5 again propagated FBS-induced *p*-ERK levels. HA-HRAS$^{Q61L}$ expression marginally increased basal and FBS-induced *p*-ERK levels, but neither *Dusp5* KO nor rescue significantly influenced responses (Fig. 6A). In contrast, HA-BRAF$^{V600E}$ expression caused high *p*-ERK signaling irrespective of FBS stimulus, and *Dusp5* deletion further elevated *p*-ERK levels by ~30%, which was dose-dependently inhibited by Ad DUSP5-Myc rescue at all time points (Fig. 6A). These data suggest that the loss of negative feedback caused by either ΔCRAF-ER or BRAF$^{V600E}$ expression is sufficient to transform the regulatory function of DUSP5, from a cytoplasmic propagator to cell-wide inhibitor of ERK (compare Fig. 4B and 6A).

In the absence of other genetic mutations, RAS$^{mut}$ or BRAF$^{V600E}$ expression can cause 'oncogene-induced' cell cycle arrest and senescence, which is mediated by hyperactivation of ERK and consequently limits cell transformation (16, 39–41). We have previously shown that *Dusp5* KO does not influence HRAS$^{Q61L}$-mediated MEF proliferation or transformation (22), but reasoned that the more pronounced effects of *Dusp5* KO on BRAF$^{V600E}$ signaling might be sufficient to mediate such changes. To test this, we performed colony formation assays in WT and *Dusp5* KO MEFs immortalized by targeted *Cdkn2a* knockdown (22) and expressing either HRAS$^{Q61L}$ or BRAF$^{V600E}$. Both oncogenes induced comparable transformation rates in WT MEFs, but *Dusp5* KO selectively abolished BRAF$^{V600E}$-driven transformation (Fig. 6B). To establish whether these effects were accompanied by a similar influence on proliferation, we compared rates of S-phase entry 24 h after addition of HA-HRAS$^{Q61L}$ or HA-BRAF$^{V600E}$. As nuclear ERK activity is required for proliferation (42) and because the effects of *Dusp5* KO on BRAF$^{V600E}$ signaling were most apparent in the nucleus, we specifically compared nuclear *p*-ERK with rates of S-phase entry. *Dusp5* KO caused a 25% increase in HA-BRAF$^{V600E}$-induced nuclear *p*-ERK and a corresponding 50% drop in S-phase positive cells (Fig. 6C). Partial blockade of *p*-ERK signaling in HA-BRAF$^{V600E}$+*Dusp5* KO cells using sub-IC$_{50}$ (0.1 μM) MEKi, completely restored rates of S-phase entry, while more complete *p*-ERK inhibition using higher MEKi concentrations (> 1 μM) caused a complete cessation of proliferation (Fig. 6C). In either control populations without oncogene or HA-HRAS$^{Q61L}$-expressing populations, *Dusp5* KO had no significant effect on nuclear *p*-ERK responses, S-phase entry or MEKi efficacy (Fig. 6C). These data are consistent with studies indicating that only a narrow range of ERK activity can promote cell cycle progression (14, 41), and suggest that *Dusp5* KO+BRAF$^{V600E}$ increases ERK activity beyond thresholds that are compatible with cell proliferation.

In order to test whether the effects of *Dusp5* deletion seen on proliferation rate reflected a particular subpopulation of cells, we compared oncogene expression versus nuclear *p*-ERK and S-

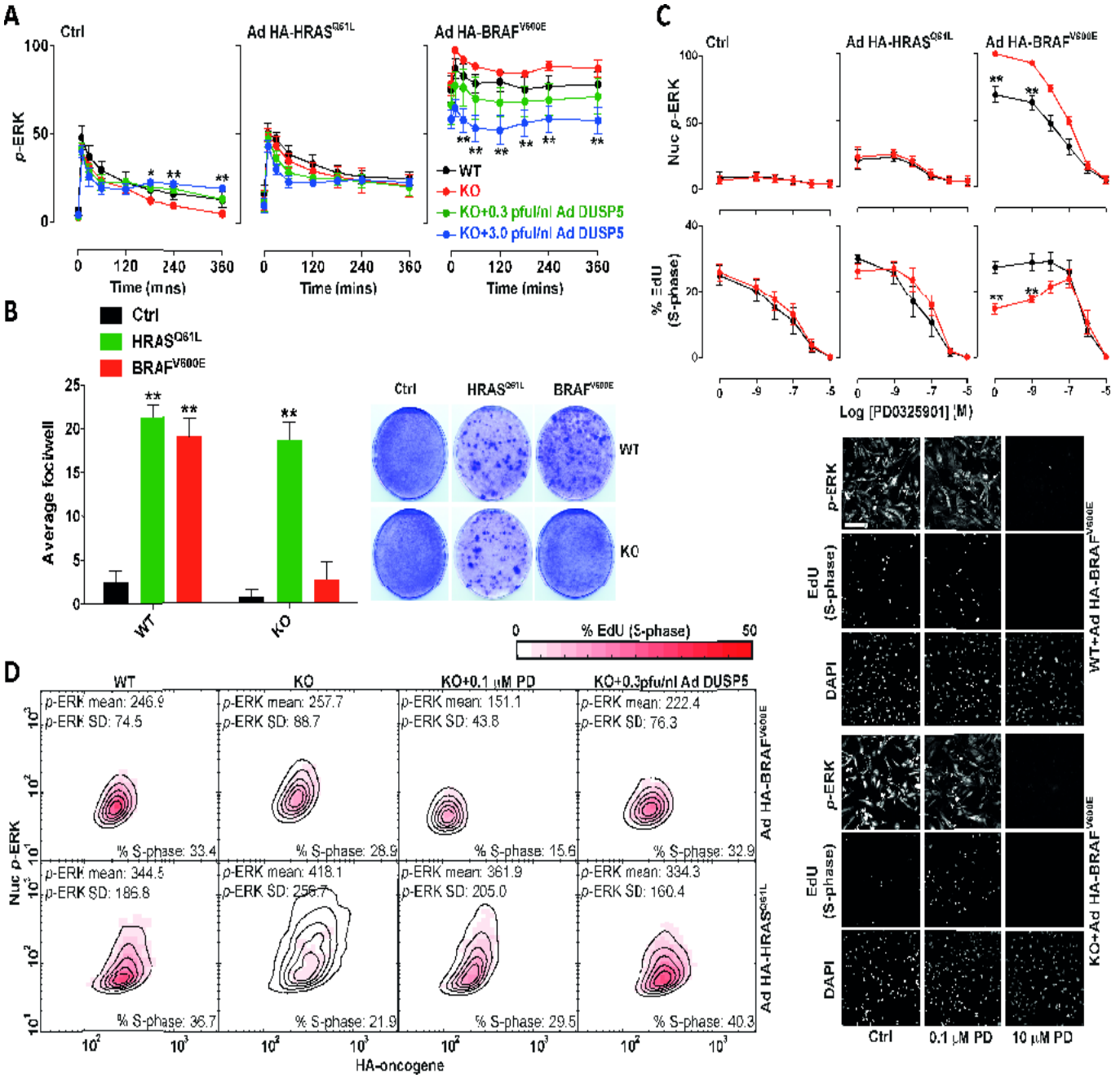


**Fig. 6.** BRAF$^{V600E}$ expression combined with *Dusp5* deletion causes ERK hyperactivation and proliferative arrest. (*A*) Primary wild-type (WT) and *Dusp5* knockout (KO) MEFs were infected with empty adenovirus (Ad), Ad HA-HRAS$^{Q61L}$ or Ad HA-BRAF$^{V600E}$ alongside 0.3-3 pfu/nl of Ad expressing *EGR1* promoter-driven DUSP5-Myc prior to stimulation with 20% FBS. Plots show time courses comparing whole-cell *p*-ERK levels using high content microscopy. Normalized population mean AFU values are shown ±SEM, n=4. *p<0.05, **p<0.01 comparing KO vs KO+3.0 pfu/nl Ad DUSP5-Myc using 2-way repeated measures ANOVA and Bonferroni post-test. (*B*) Immortalized WT and *Dusp5* KO MEFs were infected with retrovirus control, HRAS$^{Q61L}$ or BRAF$^{V600E}$ vectors for 2 weeks prior to assessment of transformed foci using methylene blue staining. Representative plate scans are shown and plots show average focus formation/well ±SEM, n=4. **p<0.01 comparing WT vs KO using 2-way repeated measures ANOVA and Bonferroni post-test. (*C*) Primary WT and *Dusp5* KO MEFs were infected with either empty Ad, Ad HA-HRAS$^{Q61L}$ or Ad HA-BRAF$^{V600E}$ and treated with increasing doses of PD0325901 MEK inhibitor for 24 h prior to a 2 h fluorescent EdU pulse label, immunostaining for *p*-ERK and analysis using high content microscopy. Plots show nuclear (Nuc) *p*-ERK levels and the percentage of EdU positive cells ±SEM, n=3. **p<0.01 using 2-way repeated measures ANOVA and Bonferroni post-test comparing WT and KO. Representative images are shown beneath. Scale bar = 200 μm. (*D*) WT and *Dusp5* KO primary MEFs were infected with Ad HA-BRAF$^{V600E}$ (top row), Ad HA-HRAS$^{Q61L}$ (bottom row) and 0.3 pfu/nl Ad DUSP5-Myc and treated with 0.1 μM PD0325901 (PD) as indicated for 24 h prior to 2 h fluorescent EdU pulse labeling of S-phase cells and counterstaining for *p*-ERK and HA-tag. The plots show HA intensity versus Nuc *p*-ERK in single cells; contour lines show equal cell density and the heat map reflects the percentage of S-phase positive cells within HA and *p*-ERK bins. Data plotted are in raw AFU and population statistics, including mean *p*-ERK levels, *p*-ERK standard deviation (SD) and overall percentage of S-phase positive cells are shown in within individual plots.

phase entry in single cells. We found that *Dusp5* deletion selectively increased nuclear *p*-ERK and reduced S-phase entry across a 10-fold difference in HA-BRAF$^{V600E}$ (but not HA-HRAS$^{Q61L}$) expression, and also increased the cell-cell heterogeneity of the

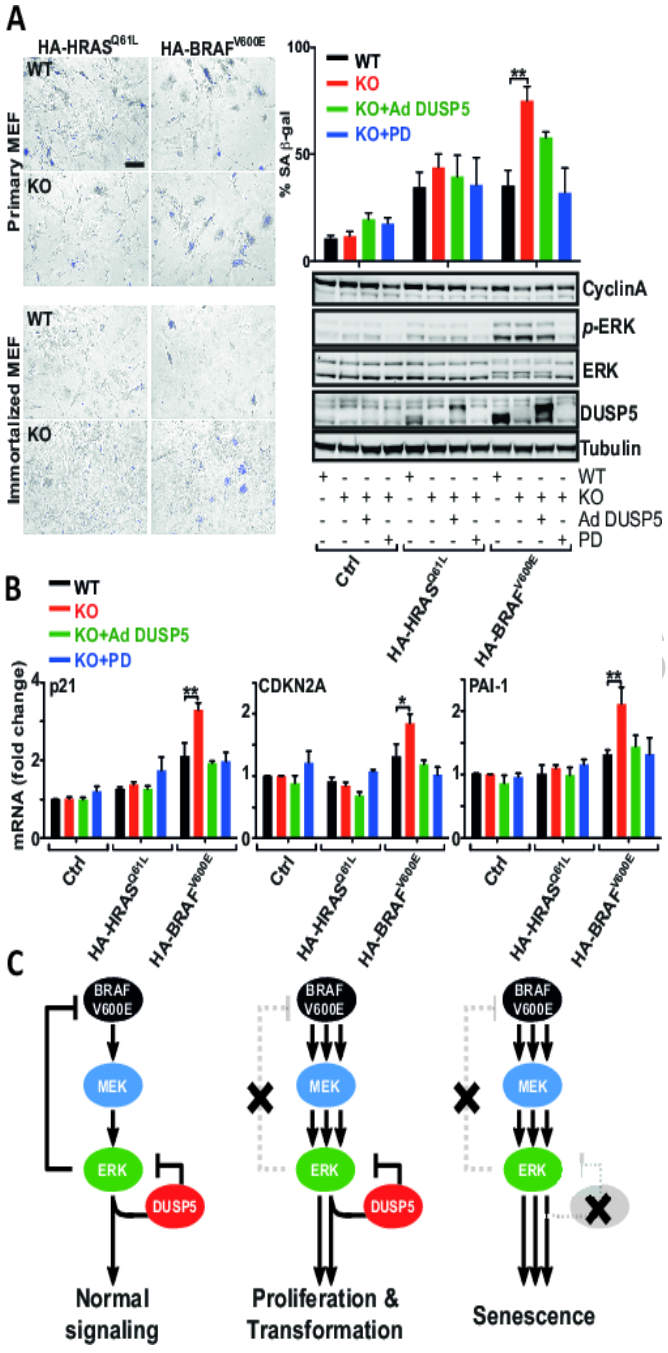


**Fig. 7.** *Dusp5* deletion accelerates BRAF$^{V600E}$-driven senescence in MEFs and cancer cell lines.(*A*) Wild-type (WT) and *Dusp5* knockout (KO) primary and immortalized MEFs were infected with empty adenovirus (Ad), Ad HA-HRAS$^{Q61L}$, Ad HA-BRAF$^{V600E}$ and Ad *EGR1*-promoter driven DUSP5-Myc (Ad DUSP5) and treated with 0.1 μM PD0325901 (PD) MEK inhibitor as indicated. Representative images show senescence-associated β–galactosidase (SA β–gal) staining of MEFs after 72 h. Scale bar = 125 μm. The quantification of SA β–gal staining is shown for primary MEFs after 72 h ±SEM, n=4. **p<0.01 using 2-way repeated measures ANOVA and Bonferroni post-test. Western blots compare indicated protein levels in primary MEFs 24 h after oncogene expression.(*B*) The plots show qPCR comparisons of indicated mRNA levels from primary MEFs treated as in (*A*) for 24 h. *p<0.05, **p<0.01 using 2-way repeated measures ANOVA and Bonferroni post-test.(*C*) Model depicting cellular consequences of combined BRAF$^{V600E}$ expression and DUSP5 deletion.

response (reflected by the increased spread of *p*-ERK histogram contours and standard deviation values; Fig. 6D). Addition of Ad DUSP5-Myc or 0.1 μM MEKi reversed the effects of *Dusp5* KO+HA-BRAF$^{V600E}$ on nuclear *p*-ERK levels, heterogeneity and S-phase response (Fig. 6C, 6D and S7). Our data therefore support a model where proliferation of cells is robust to disruption of a single feedback loop by either BRAF$^{V600E}$ expression or *Dusp5* deletion, but their combinatorial loss increases both the intensity and heterogeneity of the *p*-ERK response to such an extent that proliferation is inhibited.

**DUSP5 deletion accelerates BRAF$^{V600E}$-driven senescence.** Finally, we investigated whether DUSP5 was able to influence HRAS$^{Q61L}$ or BRAF$^{V600E}$ oncogene-induced senescence. As expected, expression of HA-BRAF$^{V600E}$ or HA-HRAS$^{Q61L}$ in primary and immortalized MEFs increased the proportion of senescence-associated β-galactosidase positive cells (SA β-Gal$^{+}$) within 72 h by ~3.5 fold (Fig. 7A). However, *Dusp5* deletion doubled the HA-BRAF$^{V600E}$-induced proportion of SA β-Gal$^{+}$ cells, which was reversed by 0.3 pfu/nl Ad DUSP5-Myc rescue or the addition of 0.1 μM MEKi (Fig. 7A), suggesting that the onset of senescence is accelerated by *Dusp5* deletion. We therefore sought to establish if molecular changes associated with senescence (39) were altered at earlier time points. Western blotting of whole cell lysates showed that HA-BRAF$^{V600E}$ expression for just 24 h in primary *Dusp5* KO MEFs caused a small, but not statistically significant, decrease in Cyclin A expression (Fig. 7A) and markedly elevated levels of *Cdkn1a* (p21$^{CIP1}$), *Cdkn2a* (p16$^{INK4A}$) and *Serpine1* (PAI-1) mRNA (Fig. 7B). All of these changes were entirely restored to levels seen in WT cells by Ad DUSP5-Myc rescue or 0.1 μM MEKi, indicating that the elevation of these senescence markers is both DUSP5- and MEK-dependent. No such changes were seen when combining *Dusp5* KO with HA-HRAS$^{Q61L}$ expression or in the absence of oncogene expression. These data collectively suggest that in this MEF model of incipient tumorigenesis, *Dusp5* deletion accelerates BRAF$^{V600E}$-induced cell cycle arrest and senescence by causing ERK hyperactivation.

## Discussion

We demonstrate that DUSP5, a phosphatase that is induced by ERK activity and specifically inactivates and anchors ERK in the nucleus (19–22), can also increase cytoplasmic ERK activation (Fig. 1). These positive effects of DUSP5 are dependent upon the relief of upstream kinase inhibition (Fig. 2 and 4), the nuclear localization of DUSP5 (Fig. 3) and rapid DUSP5 degradation (Fig. 5). Expression of the BRAF$^{V600E}$ oncogene, which is present in ~8% of all human tumors (43) and is refractory to ERK feedback inhibition (5, 26), reprograms the regulatory role of DUSP5 to facilitate cell proliferation and transformation (Fig. 6 and 7). Critically, these data show that members of the MKP/DUSP family can exert substantial effects through 'feedback relief' as a consequence of their interaction with target MAPKs. As most MKP/DUSPs have distinct MAPK substrate affinities, half-lives and promoter regulation (10, 11), our data have important consequences for understanding how the MKP/DUSPs influence MAPK signaling in different contexts, including malignant progression.

Whilst our data show that DUSP5 can propagate ERK signaling in response to sustained stimuli, such as serum, TPA or NGF (Fig. 1 and S3), it is likely that these effects are stimulus-specific. For example, it is difficult to envisage a mechanism where DUSP5 could possibly extend ERK signaling induced by transient stimuli that are desensitized before significant levels of DUSP5 have been expressed (< 60 min). We used a conceptual three-component mathematical model in our study, which mimicked the propagation of ERK signaling by DUSP5 (Fig. 4, 5 and S5A). A key predicted requirement for this signal propagation in our mathematical model is the highly non-linear inhibition of

upstream kinases by ERK (Fig. 4A). This prediction was tested in cells using expression of either a conditionally activatable ΔCRAF-ER fusion or the $BRAF^{V600E}$ oncogene, both of which disable ERK-mediated feedback inhibition of RAF (26, 30) and reversed the function of DUSP5, from propagator to inhibitor of ERK activity (Fig. 4 and 6). Our data therefore suggest that the regulatory effects of DUSP5 are profoundly dependent upon the relief of feedback between ERK and upstream kinases. Thus, signals that cause ERK activation via MEK-activating kinases other than RAF, such as Mos, MEKK1 (MAP3K1), and COT/Tpl2 (MAP3K8), which are not typically feedback inhibited by ERK (12, 44), may also reverse the function of DUSP5 in a similar manner to ΔCRAF-ER or $BRAF^{V600E}$ (Fig. 4 and 6).

The notion that DUSP5 (and likely other MKP/DUSPs) should mediate effects through 'feedback relief' is perhaps to be expected in light of the number of studies demonstrating that pharmacological inhibitors of the ERK pathway cause similar effects (25, 30, 36, 37, 45, 46). Our results indicate that the nuclear sequestration of inactive ERK by DUSP5 evokes compensatory increases in upstream RAF and MEK activation through feedback relief (Fig. 2A and S4), and that the release of ERK following DUSP5 degradation causes a rebound in ERK activity (Fig. 5). Strikingly, we found that mutation of the nuclear localization signal (NLS) of DUSP5, which impedes nuclear import (21), causes potent inhibition of ERK throughout the cell. Similar data were seen following expression of DUSP6 (a cytoplasmic paralog of DUSP5 (11)), indicating that the nuclear localization of DUSP5 is a requirement for its propagation of cytoplasmic ERK activity (Fig. 3). These data are somewhat surprising, given that the inclusion of cellular compartmentalization in our mathematical model made no difference to our *in silico* simulations of ERK signal propagation by DUSP5 (compare Fig. 4A, S5A and S5B). Our mathematical model is therefore predictive of DUSP5 behavior when it is confined to the nucleus, but cannot at present account for why cytoplasmic MKP/DUSPs may, in contrast, attenuate ERK activity so potently. Nevertheless, our experimental data clearly indicate that DUSP5 and DUSP6 play distinct roles in regulating ERK that are likely attributable to their subcellular distribution. Resolving the molecular basis for these differences will be the subject of future investigation.

Our data indicate that, despite the fact that DUSP5 can regulate both nuclear and cytoplasmic ERK signaling ((22) and Fig. 1), its deletion does not obviously influence normal cell proliferation in primary or immortalized MEFs (Fig. 6). Furthermore, mice entirely lacking DUSP5 develop normally and display no obvious adult phenotype (22), suggesting that the physiological role of DUSP5 may only be fully apparent in the event of stress or pathological challenge. In support of this, our previous data demonstrate that DUSP5 suppresses $HRAS^{Q61L}$-driven tumors in a DMBA/TPA chemical carcinogenesis model (22). Our current study also supports this view by showing that DUSP5 facilitates $BRAF^{V600E}$-driven cell proliferation and transformation by preventing ERK hyperactivation and senescence in MEFs (Fig. 6 and 7). These data may explain why DUSP5 is typically retained or even elevated in cells derived from advanced $BRAF^{V600E}$ tumors (25, 26). Our findings also support a growing body of evidence demonstrating that both normal and tumor cells are under strong selection pressure to maintain ERK activity within a narrow threshold range, such that both ERK inhibition and hyperactivation may cause tumor suppression (14, 15, 18, 41). It is therefore possible that the inhibition or loss of DUSP5 may have beneficial effects in $BRAF^{V600E}$ tumors by causing ERK hyperactivation, as has been demonstrated for DUSP6, whose inhibition or deletion causes senescence in BCR-ABL-driven adult lymphoblastic leukemia (17).

The data in our present study indicates that *Dusp5* deletion can alter MEK inhibitor efficacy (Fig. 6C). Future work will therefore focus on the possible interactions between DUSP5 and chemical inhibitors of ERK pathway components in order to better inform personalized therapy. While it is logical to test compounds already in clinical use, it will be important to also examine emerging ERK-targeted compounds that are reported to act by inhibiting ERK dimerization (47) or nuclear translocation (48), as well as explore the possibility that DUSP5-specific inhibitors may be developed. It is likely that the most effective extension of our current work will be to determine the effects of *Dusp5* loss in human cancer cell lines with different oncogenic backgrounds combined with the use of murine models that allow tissue-specific conditional expression of $BRAF^{V600E}$ combined with *Dusp5* deletion to further define the *in vivo* significance of our results. Finally, DUSP5 has recently been shown to regulate ERK-dependent gene expression and survival in eosinophils and to modulate responses to helminth infection in mice (49). The latter results indicate that the relevance of our work may extend beyond the regulation of oncogenic signaling to other diseases in which abnormal ERK activity has been implicated. These include inflammatory disease, cardiac hypertrophy, metabolic disorders and neurodegenerative conditions, such as Alzheimer's disease (50–53).



## Experimental Procedures

**Cell Culture and Viral Infection.** Primary and immortalized MEFs were derived and cultured as previously described (22). PC12 cells (a kind gift from Dr. Shelley Allen, University of Bristol, UK) were maintained in RPMI 1640 medium containing GlutaMAX (Invitrogen), 5% horse serum (Invitrogen) and 10% fetal bovine serum (Invitrogen) in flasks coated with type I collagen from rat tail (Sigma). For experiments, cells were infected with Ad vectors for 4-6 h.

**High Content Microscopy and Analysis.** Cells were immunostained in 96-well black-wall imaging plates (Corning, 3904) as previously described (22) and imaged using an IN Cell Analyzer 2000 (GE Healthcare) microscope using a 10x or 20x objective lens, typically acquiring 500-2000 individual cells (2-6 fields) per well in duplicate or triplicate wells per condition. All exposures were set such that signals were >30 AFU above background and maximal <500 AFU below the maximum dynamic range. S-phase pulse labeling experiments were carried out using 10 μM EdU fluorescent thymidine analog (5-ethynyl-2'-deoxyuridine, EdU) for 2 h prior to cell fixation and detected using a Click-iT® EdU Alexa Fluor® 647 HCS Assay kit (Invitrogen), according to manufacturer's instructions. In multiplex assays, EdU Alexa Fluor® 647 detection was carried out prior to antibody staining. Analysis was performed using IN Cell Developer software (GE Healthcare) and a custom algorithm using DAPI and *p*-ERK images to define nuclear and cytoplasmic regions, respectively, which were used as a binary mask applied to images from all fluorophores to derive measures on a per cell, per compartment basis.

Details of all other methodology used, including vector manufacture and mathematical modeling, are detailed in SI Materials and Methods.

**Author Contributions**

CJC and SK conceived the study; TR, CJC and SK obtained funding; AK, LR, TR, SK and CJC designed experiments; AK, LR, JS, JD, EC, TR and CJC carried out experiments and analyzed data; CJC, JS, JD, CAB, CJB, LR and AK created tools and reagents; AK, CJC and SK wrote the manuscript.

**Acknowledgements**

We thank Dr. Simon Cook, (Babraham Institute), Dr Susanne Gebhard (University of Bath), Dr. Owen Sansom (Beatson Institute) and Dr. Albena Dinkova-Kostova (University of Dundee) for critical reading of the MS. This work was supported by a Cancer Research UK Programme Grant (C8227/A12053) to SK, a Royal Society Research Grant (2010/R2) to CJC, an MRC Research Grant to SK and CJC (MR/N020790/1), a Dundee Cancer Centre Studentship to AK and a Commonwealth Scholarship to CAB. TR gratefully acknowledges the support of the Royal Society.

1. Ebisuya M, Kondoh K, Nishida E (2005) The duration, magnitude and compartmentalization of ERK MAP kinase activity: mechanisms for providing signaling specificity. *J Cell Sci* 118(Pt 14):2997–3002.
2. Marshall CJ (1995) Specificity of receptor tyrosine kinase signaling: transient versus sustained extracellular signal-regulated kinase activation. *Cell* 80(2):179–85.
3. Lavoie H, Therrien M (2015) Regulation of RAF protein kinases in ERK signalling. *Nat Rev Mol Cell Biol* 16(5):281–298.
4. Dougherty MK, et al. (2005) Regulation of Raf-1 by direct feedback phosphorylation. *Mol*

*Cell* 17(2):215–24.
5. Ritt DA, Monson DM, Specht SI, Morrison DK (2010) Impact of feedback phosphorylation and Raf heterodimerization on normal and mutant B-Raf signaling. *Mol Cell Biol* 30(3):806–19.
6. Rushworth LK, Hindley AD, O'Neill E, Kolch W (2006) Regulation and Role of Raf-1 / B-Raf Heterodimerization. *Mol Cell Biol* 26(6):2262.
7. Buday L, Warne PH, Downward J (1995) Downregulation of the Ras activation pathway by MAP kinase phosphorylation of Sos. *Oncogene* 11(7):1327–31.
8. Zakrzewska M, et al. (2013) ERK-Mediated Phosphorylation of Fibroblast Growth Factor Receptor 1 on Ser 777 Inhibits Signaling. *Sci Signal* 6(262):ra11.
9. Li X, Huang Y, Jiang J, Frank SJ (2008) ERK-dependent threonine phosphorylation of EGF receptor modulates receptor downregulation and signaling. *Cell Signal* 20(11):2145–55.
10. Caunt CJ, Keyse SM (2013) Dual-specificity MAP kinase phosphatases (MKPs): shaping the outcome of MAP kinase signalling. *FEBS J* 280(2):489–504.
11. Owens DM, Keyse SM (2007) Differential regulation of MAP kinase signalling by dual-specificity protein phosphatases. *Oncogene* 26(22):3203–13.
12. Caunt CJ, Sale MJ, Smith PD, Cook SJ (2015) MEK1 and MEK2 inhibitors and cancer therapy: the long and winding road. *Nat Rev Cancer* 15(10):577–592.
13. Kidger AM, Keyse SM (2016) The regulation of oncogenic Ras/ERK signalling by dual-specificity mitogen activated protein kinase phosphatases (MKPs). *Semin Cell Dev Biol* 50:125–132.
14. Das Thakur M, et al. (2013) Modelling vemurafenib resistance in melanoma reveals a strategy to forestall drug resistance. *Nature* 494(7436):251–5.
15. Sun C, et al. (2014) Reversible and adaptive resistance to BRAF(V600E) inhibition in melanoma. *Nature* 508(7494):118–122.
16. Deschênes-Simard X, Kottakis F, Meloche S, Ferbeyre G (2014) ERKs in cancer: friends or foes? *Cancer Res* 74(2):412–9.
17. Shojaee S, et al. (2015) Erk Negative Feedback Control Enables Pre-B Cell Transformation and Represents a Therapeutic Target in Acute Lymphoblastic Leukemia. *Cancer Cell* 28:1–15.
18. Moriceau G, et al. (2015) Tunable-Combinatorial Mechanisms of Acquired Resistance Limit the Efficacy of BRAF/MEK Cotargeting but Result in Melanoma Drug Addiction. *Cancer Cell* 27(2):240–256.
19. Buffet C, et al. (2015) Dual Specificity Phosphatase 5, a Specific Negative Regulator of ERK Signaling, Is Induced by Serum Response Factor and Elk-1 Transcription Factor. *PLoS One* 10(12):e0145484.
20. Kucharska A, Rushworth LK, Staples CJ, Morrice NA, Keyse SM (2009) Regulation of the inducible nuclear dual-specificity phosphatase DUSP5 by ERK MAPK. *Cell Signal* 21(12):1794–805.
21. Mandl M, Slack DN, Keyse SM (2005) Specific inactivation and nuclear anchoring of extracellular signal-regulated kinase 2 by the inducible dual-specificity protein phosphatase DUSP5. *Mol Cell Biol* 25(5):1830–1845.
22. Rushworth LK, et al. (2014) Dual-specificity phosphatase 5 regulates nuclear ERK activity and suppresses skin cancer by inhibiting mutant Harvey-Ras (HRasQ61L)-driven SerpinB2 expression. *Proc Natl Acad Sci U S A* 111(51):18267–18272.
23. Shin SH, Park SY, Kang GH (2013) Down-regulation of dual-specificity phosphatase 5 in gastric cancer by promoter CpG island hypermethylation and its potential role in carcinogenesis. *Am J Pathol* 182(4):1275–1285.
24. Cai C, et al. (2015) Down-regulation of dual-specificity phosphatase 5 predicts poor prognosis of patients with prostate cancer. *Int J Clin Exp Med* 8(3):4186–94.
25. Montero-Conde C, et al. (2013) Relief of feedback inhibition of HER3 transcription by RAF and MEK inhibitors attenuates their antitumor effects in BRAF-mutant thyroid carcinomas. *Cancer Discov* 3(5):520–33.
26. Pratilas CA, et al. (2009) (V600E)BRAF is associated with disabled feedback inhibition of RAF-MEK signaling and elevated transcriptional output of the pathway. *Proc Natl Acad Sci U S A* 106(11):4519–24.
27. Yun J, et al. (2009) Glucose deprivation contributes to the development of KRAS pathway mutations in tumor cells. *Science* 325(5947):1555–9.
28. Volmat V, Camps M, Arkinstall S, Pouysségur J, Lenormand P (2001) The nucleus, a site for signal termination by sequestration and inactivation of p42/p44 MAP kinases. *J Cell Sci* 114(Pt 19):3433–3443.
29. Nakakuki T, et al. (2010) Ligand-Specific c-Fos Expression Emerges from the Spatiotemporal Control of ErbB Network Dynamics. *Cell* 141(5):884–896.
30. Sturm OE, et al. (2010) The Mammalian MAPK/ERK Pathway Exhibits Properties of a Negative Feedback Amplifier. *Sci Signal* 3(153):ra90-ra90.
31. Omerovic J, Clague MJ, Prior IA (2010) Phosphatome profiling reveals PTPN2, PTPRJ and PTEN as potent negative regulators of PKB/Akt activation in Ras-mutated cancer cells. *Biochem J* 426(1):65–72.
32. Ekerot M, et al. (2008) Negative-feedback regulation of FGF signalling by DUSP6/MKP-3 is driven by ERK1/2 and mediated by Ets factor binding to a conserved site within the DUSP6/MKP-3 gene promoter. *Biochem J* 412(2):287–298.
33. Groom LA, Sneddon AA, Alessi DR, Dowd S, Keyse SM (1996) Differential regulation of the MAP, SAP and RK/p38 kinases by Pyst1, a novel cytosolic dual-specificity phosphatase. *EMBO J* 15(14):3621–32.
34. Karlsson M, Mathers J, Dickinson RJ, Mandl M, Keyse SM (2004) Both nuclear-cytoplasmic shuttling of the dual specificity phosphatase MKP-3 and its ability to anchor MAP kinase in the cytoplasm are mediated by a conserved nuclear export signal. *J Biol Chem* 279(40):41882–41891.
35. Marchetti S, et al. (2005) Extracellular Signal-Regulated Kinases Phosphorylate Mitogen-Activated Protein Kinase Phosphatase 3 / DUSP6 at Serines 159 and 197 , Two Sites Critical for Its Proteasomal Degradation. *Mol Cell Biol* 25(2):854–864.
36. Fritsche-Guenther R, et al. (2011) Strong negative feedback from Erk to Raf confers robustness to MAPK signalling. *Mol Syst Biol* 7(489):489.
37. Jensen KJ, Moyer CB, Janes KA (2016) Network Architecture Predisposes an Enzyme to Either Pharmacologic or Genetic Targeting. *Cell Syst* 2(2):112–121.
38. Samuels ML, Weber MJ, Bishop JM, McMahon M (1993) Conditional transformation of cells and rapid activation of the mitogen-activated protein kinase cascade by an estradiol-dependent human raf-1 protein kinase. *Mol Cell Biol* 13(10):6241–52.
39. Serrano M, Lin AW, Mccurrach ME, Beach D, Lowe SW (1997) Oncogenic ras Provokes Premature Cell Senescence Associated with Accumulation of p53 and p16 INK4a. *Cell* 88:593–602.
40. Zhu J, Woods D, McMahon M, Bishop JM (1998) Senescence of human fibroblasts induced by oncogenic Raf Senescence of human fibroblasts induced by oncogenic Raf. *Genes Dev*:2997–3007.
41. Woods D, et al. (1997) Raf-induced proliferation or cell cycle arrest is determined by the level of Raf activity with arrest mediated by p21Cip1. *Mol Cell Biol* 17(9):5598–611.
42. Brunet A, et al. (1999) Nuclear translocation of p42/p44 mitogen-activated protein kinase is required for growth factor-induced gene expression and cell cycle entry. *EMBO J* 18(3):664–674.
43. Davies H, et al. (2002) Mutations of the BRAF gene in human cancer. *Nature* 417(6892):949–54.
44. Cuevas BD, Abell AN, Johnson GL (2007) Role of mitogen-activated protein kinase kinase kinases in signal integration. *Oncogene* 26(22):3159–71.
45. Friday BB, et al. (2008) BRAF V600E disrupts AZD6244-induced abrogation of negative feedback pathways between extracellular signal-regulated kinase and Raf proteins. *Cancer Res* 68(15):6145–53.
46. Lito P, et al. (2012) Relief of Profound Feedback Inhibition of Mitogenic Signaling by RAF Inhibitors Attenuates Their Activity in BRAFV600E Melanomas. *Cancer Cell* 22(5):668–682.
47. Herrero A, et al. (2015) Small Molecule Inhibition of ERK Dimerization Prevents Tumorigenesis by RAS-ERK Pathway Oncogenes. *Cancer Cell* 28(2):170–182.
48. Michailovici I, et al. (2014) Nuclear to cytoplasmic shuttling of ERK promotes differentiation of muscle stem/progenitor cells. *Development* 141:1–10.
49. Holmes DA, Yeh J, Yan D, Xu M, Chan AC (2014) Dusp5 negatively regulates IL-33-mediated eosinophil survival and function. *EMBO J* 34(2):218–35.
50. Sabio G, Davis RJ (2014) TNF and MAP kinase signalling pathways. *Semin Immunol* 26(3):237–245.
51. Diamanti-Kandarakis E, Dunaif A (2012) Insulin resistance and the polycystic ovary syndrome revisited: An update on mechanisms and implications. *Endocr Rev* 33(6):981–1030.
52. Subramaniam S, Unsicker K (2010) ERK and cell death: ERK1/2 in neuronal death. *FEBS J* 277(1):22–29.
53. Lorenz K, Schmitt JP, Vidal M, Lohse MJ (2009) Cardiac hypertrophy: Targeting Raf/MEK-/ERK1/2-signaling. *Int J Biochem Cell Biol* 41(12):2351–2355.
54. Caunt CJ, McArdle CA (2010) Stimulus-induced uncoupling of extracellular signal-regulated kinase phosphorylation from nuclear localization is dependent on docking domain interactions. *J Cell Sci* 123(Pt 24):4310–20.
55. Anderson RD, Haskell RE, Xia H, Roessler BJ, Davidson BL (2000) A simple method for the rapid generation of recombinant adenovirus vectors. *Gene Ther* 7(12):1034–1038.
56. Staples CJ, Owens DM, Maier J V, Cato ACB, Keyse SM (2010) Cross-talk between the p38alpha and JNK MAPK pathways mediated by MAP kinase phosphatase-1 determines cellular sensitivity to UV radiation. *J Biol Chem* 285(34):25928–40.
57. Kidger A, et al. (2016) Data from "DUSP5 controls the localized inhibition, propagation and transforming potential of ERK signalling." *Univ Bath*. doi:https://doi.org/10.15125/BATH-0-0317.
58. Lidke DS, et al. (2010) ERK nuclear translocation is dimerization-independent but controlled by the rate of phosphorylation. *J Biol Chem* 285(5):3092–3102.